Current-induced domain wall motion in permalloy nanowires with a rectangular cross-section

J. H. Ai, B. F. Miao, L. Sun, B. You, An Hu, and H. F. Ding

Citation: J. Appl. Phys. **110**, 093913 (2011); doi: 10.1063/1.3658219
View online: http://dx.doi.org/10.1063/1.3658219
View Table of Contents: http://aip.scitation.org/toc/jap/110/9
Published by the American Institute of Physics

Current-induced domain wall motion in permalloy nanowires with a rectangular cross-section

J. H. Ai, B. F. Miao, L. Sun,[a] B. You, An Hu, and H. F. Ding[b]
National Laboratory of Solid State Microstructures and Department of Physics, Nanjing University, 22 Hankou Rd., Nanjing 210093, China

(Received 14 August 2011; accepted 29 September 2011; published online 8 November 2011)

We performed micromagnetic simulations of the current-induced domain wall motion in permalloy nanowires with rectangular cross-section. In the absence of the nonadiabatic spin-transfer term, a threshold current, J_c is required to drive the domain wall moving continuously. We find that J_c is proportional to the maximum cross product of the demagnetization field and magnetization orientation of the domain wall and the domain wall width. With varying both the wire thickness and width, a minimum threshold current in the order of 10^6 A/cm^2 is obtained when the thickness is equivalent to the wire width. With the nonadiabatic spin-transfer term, the calculated domain wall velocity v equals to the adiabatic spin transfer velocity u when the current is far above the Walker limit J_w. Below J_w, $v = \frac{\beta}{\alpha}u$, where β is the nonadiabatic parameter and α is the damping factor. For different β, we find the Walker limit can be scaled as $J_w = \frac{\alpha}{|\beta-\alpha|}J_c$. Our simulations agree well with the one dimensional analytical calculation, suggesting the findings are the general behaviors of the systems in this particular geometry. © *2011 American Institute of Physics*. [doi:10.1063/1.3658219]

I. INTRODUCTION

A ferromagnet typically contains a number of small regions called domains, within each of which the local moments align. The adjacent domains are separated by a domain wall (DW), in which the direction of moments gradually changes. To make the DW travel in a ferromagnet, conventionally a magnetic field is required. An alternative way to drive DW motion is to supply an electrical current. The current-induced DW motion[1,2] in magnetic nanowires has attracted much attentions both experimentally[3–9] and theoretically.[10–15] Based on current-induced DW motion, a new type of memory, the racetrack memory has been proposed by Parkin.[3] In a racetrack memory, magnetic domains are used to store information in tall columns of magnetic material arranged perpendicularly on the surface of a wafer. In such configuration, the storage capacity can be significantly increased as the information is stored three-dimensionally. The racetrack memory also requires less energy in comparison with traditional hard disk techniques as it has no mechanically moving parts. To be technologically practicable, magnetic domains need to be manipulated easily, and the velocity of DW motion should be large enough at relatively low current density. The threshold current density which is needed to move the DW, however, is found to be in the order of 10^8 A/cm^2, which is still much too large.[3–8] In this paper, we perform micromagnetic simulations of the current-induced DW motion in permalloy (Py) nanowires to explore the relationship between the threshold current density and the shape parameters of the nanowire and to find the potential ways to decrease the threshold current density. We find the threshold current can be strongly reduced to be in the order of 10^6 A/cm^2 when the nanowire thickness is equivalent to its width. With the nonadiabatic spin-transfer term, the calculated domain wall velocity v equals to the adiabatic spin transfer velocity u when the current density is far above the Walker limit J_w. Below J_w, $v = \frac{\beta}{\alpha}u$, where β is the nonadiabatic parameter and α is the damping factor. For different β, we find the Walker limit can be scaled as $J_w = \frac{\alpha}{|\beta-\alpha|}J_c$. Our simulations agree well with the one dimensional analytical calculation,[13] suggesting the findings are the general behaviors of the systems in this particular geometry.

II. SIMULATION DETAILS

The micromagnetic simulations are performed within the framework of OOMMF codes[16] with extensions of the current induced magnetization dynamics.[17] When the current is along the x-axis, it can be described by the Gilbert equation with additional spin transfer torque terms,[12,13] i.e.,

$$\frac{d\mathbf{m}}{dt} = |\gamma|\mathbf{H}_{eff} \times \mathbf{m} + \alpha\mathbf{m} \times \frac{d\mathbf{m}}{dt} + \mathbf{u}\cdot\mathbf{m} \times \left(\mathbf{m} \times \frac{\partial\mathbf{m}}{\partial x}\right) + \beta\mathbf{u}\cdot\mathbf{m} \times \frac{\partial\mathbf{m}}{\partial x}, \quad (1)$$

where $\mathbf{m}$ is the unit magnetization, γ is the gyromagnetic ratio, $\mathbf{H}_{eff}$ is the effective field, and α is the Gilbert damping factor. The first two terms on the right side describe the spin dynamics without the electrical current. To accommodate the spin transfer torque effect, a velocity $\mathbf{u}$ (adiabatic spin transfer velocity) is introduced. It is a vector directed along the direction of electron motion with an amplitude $u = JPg\mu_B/2eM_s$, where J is the current density, P is the spin polarization of the current, g is the Lande factor, μ_B is the Bohr magneton, e is the electron charge, and M_s is the saturation magnetization. β is the parameter used to describe the nonadiabatic spin transfer torque. In our simulations, the

[a]Electronic mail: lsun@nju.edu.cn.
[b]Electronic mail: hfding@nju.edu.cn.

current is assumed to align along the wire axis. The material parameters of bulk Py, i.e., the saturation magnetization $M_s = 8 \times 10^5$ A/m, the exchange constant $A = 1.3 \times 10^{-11}$ J/m, the spin polarization $P = 0.4$ and zero anisotropy are used in our simulations.[18,19] The calculations are carried out in 3-dimensional mode. As the exchange length of Py is about 5 nm, we chose the size of the mesh to be 2 nm in each direction. To check the precision, we also compared some results (mainly for small samples) with the data obtained with the mesh size of 1 nm in each direction and did not find any change in our main results.

III. RESULTS AND DISCUSSION

Fig. 1 shows the schematic diagram for different types of DW in the nanowires, (a) transverse wall, (b) perpendicular transverse wall, and (c) antivortex wall, respectively. For the nanowire with the transverse wall, the wire is along x-axis and the magnetizations inside the DW are lying in the x-y plane. As the electrical current is applied along $-x$ direction in our simulations, the DW moves towards $+x$ direction, i.e., the electron flow direction. The length of the wire is chosen to be 8 μm and the threshold current density is investigated as the function of both the wire width and thickness. The consequences of Eq. (1) on the dynamics of a transverse wall with $\beta = 0$ have been studied qualitatively.[1,10] Using the integrated equations for the DW dynamics,[20,21] it was found that two cases exist. For the low current density, the spin transfer torque is counteracted by an internal restoring torque and the DW is canted out of x-y plane.[22] In such case, the DW does not move steadily under the applied current. Above a threshold, the spin transfer torque can overcome the internal torque and the DW can move continuously. When the DW is moving forward, it is also accompanied by a continuous precession of the DW. When the wire has a small width, the DW rotates as the process shown in Fig. 1: $a \rightarrow b \rightarrow \bar{a} \rightarrow \bar{b}$, while the bar stands for the π rotation around the x-axis.[13] The transverse DW typically occurs in the wires with narrow width. When the wire is considerably wide compared to the exchange length (≈ 5 nm for Py), the perpendicular DW shown in Fig. 1(b) will become unstable and the wall changes into the antivortex wall shown in Fig. 1(c). For Py, we find the antivortex wall typically appears when the wire width is larger than 16 nm.

For simplicity, we first discuss the situation for $\beta = 0$, i.e., the nonadiabatic spin transfer torque is absent. In our simulations, α is chosen to be 0.02. In order to find the threshold current density, we performed simulations for the DW movement as a function of time for various current densities. Fig. 2 shows the DW position as a function of time for the current densities just below and slightly above the threshold. The dashed line shows the simulated result for the current density just below the threshold (20.5×10^8 A/cm^2). We can find that the DW initially moves fast, and travels more than 100 nm within a few ns. After traveling for a maximum distance of about 180 nm, the DW however becomes steady. With slightly increasing the current density to 20.6×10^8 A/cm^2 (solid line), one can find that the DW can move forward continuously even though the time dependent position of the DW has a step-like behavior. Based on these results, the critical current density is determined. The inaccuracy of the simulation can be obtained from the difference between these two current densities. The step-like behavior for the time dependent DW displacement is caused by the accompanied DW rotation around the wire axis during the DW moving forward process. The periodical rotation of the DW leads to the periodical change of the linear velocity of the DW. The detailed discussion will be given below.

Fig. 3(a) shows the critical current density as a function of the wire width for the wires with 2 nm thickness. The threshold current monotonously increases with the increase of wire width but not linearly. The increasing rate reduces as the wire width increases. To understand this dependence, we also plot it as a function of the DW width, as shown in Fig. 3(b). DW width is one of the crucial parameters in current-induced DW motion. It is predicted that the critical current density is proportional to the DW width,[10,23] and the nonadiabatic spin transfer parameter β is also sensitive to the DW width.[10,24,25] In addition, the DW width can also changes with the wire width.[26,27] Indeed, we find the DW width monotonously increases with the wire width as shown in the inset in Fig. 3(b). Particularly, it shows an almost linear dependence when the wire width is above 15 nm. The width of the DW changes from about 20 nm to 60 nm for wire width from 4 nm to 50 nm. The threshold current monotonously increases with the increase of DW width, but not as linearly as predicted.[10,23] This may be related to the change of the demagnetization field when the wire width is

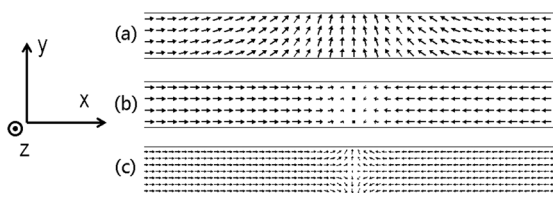

FIG. 1. Schematic different domain wall structures in a soft nanowire. (a) Transverse wall, (b) perpendicular transverse wall, and (c) antivortex wall. Each arrow represents an area of 2 nm×2 nm.

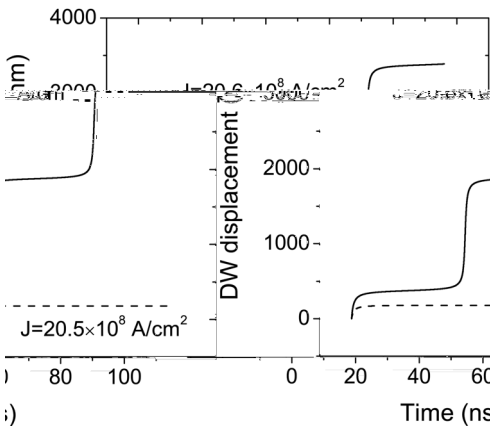

FIG. 2. Typical DW position as a function of time for two different current densities. Dashed line for current density of 20.5×10^8 A/cm^2, which is not sufficient to move the DW. Solid line for current density of 20.6×10^8 A/cm^2, which is slightly more than enough to move the DW.

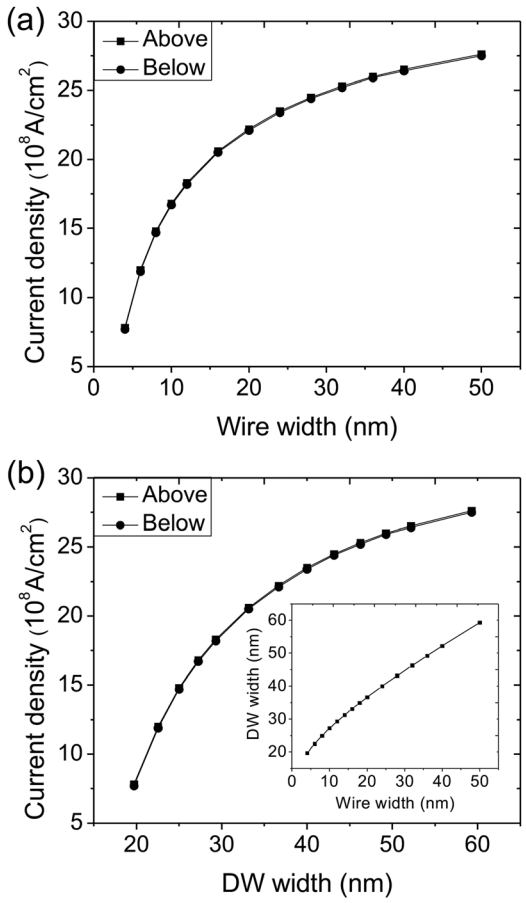

FIG. 3. Critical current density as a function of wire width (a) and the DW width (b). The circles are the current densities that are slightly below J_c while the squares are the current densities that are slightly above J_c. The thickness is 2 nm for all nanowires. Inset: DW width as a function of the wire width.

varied. According to Eq. (1), the main driving force that moves the DW forward is the adiabatic spin transfer torque term, i.e., the third term in Eq. (1), $u \cdot \mathbf{m} \times \left(\mathbf{m} \times \frac{\partial \mathbf{m}}{\partial x}\right)$. It is proportional to the product of the current density J and the gradient of magnetization along the x direction $\frac{\partial \mathbf{m}}{\partial x}$. In a linear assumption, $\frac{\partial \mathbf{m}}{\partial x}$ is inversely proportional to the DW width D_w. When the DW is traveling forward, however, the DW also rotates around the x-axis as discussed above. The first term in Eq. (1), $|\gamma|\mathbf{H}_{eff} \times \mathbf{m}$, is the precession term. In the absence of the external field, $\mathbf{H}_{eff}$ mainly consists of the demagnetization field providing that the magnetic field generated by the current can be neglected. Therefore, it can have a non-zero value when the DW tilts out of x-y plane. If we define ϕ as the angle between the x-y plane and the plane where the DW lies, the direction of the precession term will change with ϕ. The direction of this vector will be parallel or antiparallel to the adiabatic spin transfer torque depends on ϕ, which leads to the effects that the DW velocity, as well as the time dependent DW movement have a periodic change as shown in Fig. 2. The magnitude of the precession term also changes as ϕ changes and it has a maximum value at a certain angle ϕ_0. The magnitude of the adiabatic spin transfer torque is a constant for a given current. If it is smaller than the maximum value of the precession term, the DW motion will stop because the adiabatic spin transfer torque will be counteracted by the procession term when they are antiparallel. Only in the case that the adiabatic spin transfer torque exceeds the maximum value of the procession term, the DW can be continuously moved forward by the electrical current. Therefore, the threshold current density J_c is related with the maximum of the precession term. In such case, we can derive the condition for obtaining J_c, namely, $|\gamma \mathbf{H}_{demag} \times \mathbf{m}|_{max} = \left|u \cdot \mathbf{m} \times \left(\mathbf{m} \times \frac{\partial \mathbf{m}}{\partial x}\right)\right|$, where $\mathbf{H}_{demag}$ is the demagnetization field induced during the domain wall rotation. As $\frac{\partial \mathbf{m}}{\partial x}$ is inversely proportional to the DW width D_w and current density J is proportional to u, we can derive the critical current density. By neglecting a few constants, it can be written as

$$J_c \propto |\mathbf{H}_{demag} \times \mathbf{m}|_{max} D_w / P. \tag{2}$$

From above discussion, it is clear that the threshold current J_c in current-induced DW motion is mainly determined by $|\mathbf{H}_{demag} \times \mathbf{m}|_{max} D_w$. When taking the simplest approximation that the demagnetization field can be estimated from the surface magnetic dipolar charges and it is inversely proportional to the distance between two surfaces, we can easily derive that $|\mathbf{H}_{demag} \times \mathbf{m}|_{max}$ appears when the domain wall is 45° tilted away from the x-y plane and Eq. (2) can be simplified as $J_c \propto \left|\frac{1}{t} - \frac{1}{w}\right| D_w$ if the domain wall is kept as a transverse wall during its rotation. One can expect that the critical current density will dramatically decrease when the wire thickness w equals to its thickness t. To verify this, we performed the simulation for the threshold current density as a function of the nanowire thickness. The simulated results are shown in Fig. 4 for nanowires with the fixed width of 16 nm. We find that the threshold current first reduces, reaching a minimum when the wire thickness equals to its width and increases with the thickness further increases, which is consistent with the expectation. The simulated minimum of the threshold current is in the order of 10^6 A/cm^2, which is about 3 orders of magnitude smaller than the value for nanowire with thickness of 2 nm. The calculated non-zero J_c for the nanowires with square cross-section may be related to the simplified approximation we took. One may also consider using a modified 1-d model with the demagnetization form

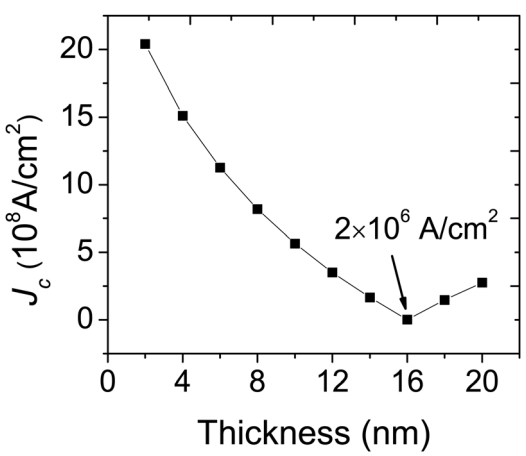

FIG. 4. Calculated critical current density as a function of the nanowire thickness. The width of the wires is 16 nm.

factor to represent the demagnetization field for the calculation of the threshold current if the domain wall is a rigid transverse wall. In our simulations, we did often observe the domain wall changing its format during its propagation process. In such situations, the 3-d simulations as described in this paper are needed.

Experimentally, similar result was also observed. Koyama *et al*. found J_c has a minimum when they change the wire width for a perpendicular magnetized nanowire.[29] For a perpendicular magnetized nanowire, the domain wall changes between a Bloch wall and Néel wall during the propagation of the domain wall and the minimum J_c appears when the energies of both types of domain wall are the same, as explained by the authors. The significant reduction of J_c for the nanowires with square cross-section is similar to case in a cylindrical wire.[28] In a cylindrical wire, the DW will move steady under a current, the velocity is proportional to the current density, and no threshold exists. For a cylindrical wire, the demagnetization field is always in the plane where the DW lies. In such configuration, the cross product of the demagnetization field and the DW magnetization is zero and makes no contribution to the DW displacement.

Above, we focus our discussion for the situation without the nonadiabatic term, i.e., $\beta = 0$. When $\beta \neq 0$, the nonadiabatic term $\beta \cdot u \cdot \mathbf{m} \times \frac{\partial \mathbf{m}}{\partial x}$ need to be considered in the calculation. We find the nonadiabatic term is always antiparallel to the damping term $\alpha \mathbf{m} \times \frac{d\mathbf{m}}{dt}$ in the geometry we discussed. The effects of both terms cause the domain wall rotate around the axis of the wire, even though the rotation direction is opposite. The competition of them determines the direction of the DW rotation, either clockwise or anticlockwise. For a certain wire, $\frac{\partial \mathbf{m}}{\partial x}$ is fixed, and $\left|\frac{d\mathbf{m}}{dt}\right|$ can be written as $\left|\frac{\partial \mathbf{m}}{\partial x}\frac{\partial x}{\partial t}\right|$, hence it is proportional to the velocity of the DW, v. Therefore, the nonadiabatic torque is only proportional to β and u while the damping term is proportional to v and the Gilbert damping factor α. When a small current J (below the Walker limit) is applied, the DW initially lies in the x-y plane and $\mathbf{H}_{demag} \times \mathbf{m} = 0$, which means no resistance force exists. In such case, the DW will initially move forward with a velocity of u. Our simulation also confirms this result, as the initial speeds are the same for different currents in Fig. 2, despite the DW stops moving for one current and keeps going for the other current. As the DW starts moving, the damping term will have a non-zero value due to the rotation of the domain wall. This non-zero demagnetization field will decelerate or accelerate the DW movement, depending on the rotation direction. When β is fixed, the value of the nonadiabatic term will be a constant for a fixed current J. When $\beta < \alpha$, the nonadiabatic term is initially smaller than the damping term, the DW will rotate to the same direction as the situation for $\beta = 0$, leading to a decelerating effect for DW. As the DW velocity decreases, the value of the damping term will decrease too, till it equals to the nonadiabatic term. In such situation, a balance between these two terms can be achieved, and the DW will stop rotating and only move forward with a constant velocity v. Vice versa, when $\beta > \alpha$, the DW will initially rotate towards the opposite direction as the situation for $\beta = 0$ and causing an accelerating effect for the DW until the speed reach v. With this, we can derive the condition for obtaining the steady velocity v under this current, namely, $\left|\beta \cdot u \cdot \mathbf{m} \times \frac{\partial \mathbf{m}}{\partial x}\right| = \left|\alpha \mathbf{m} \times \frac{d\mathbf{m}}{dt}\right|$. As $\left|\frac{d\mathbf{m}}{dt}\right| = \left|v\frac{\partial \mathbf{m}}{\partial x}\right|$, we can find that

$$v = \beta u/\alpha. \tag{3}$$

Indeed, we find that the simulated domain wall velocity (Fig. 5(a)) agrees well with this equation when the applied current density is below the Walker limit. The fact that domain wall moves with a constant speed, v, despite its initial speed u is due to the processing term forces this change when the domain wall rotates away from x-y plane to a certain angle. As both v and u increase linearly with the current J, the difference between them also increases linearly with J. The processing term, however, has a certain limit due to the fact that it is proportional to $\mathbf{H}_{eff} \times \mathbf{m}$. When the current is above a threshold (known as the Walker limit[7,8,30–32]), the processing term will be not sufficient to force this speed change. In such case, the domain wall starts rotating. With higher the current, the effect of the processing term is less important and the speed of the DW will be closer to the speed of u (The only exception is the case for $\beta = \alpha$ where the steady velocity v equals to the initial speed u and the DW will always lie in the x-y plane, and there is no DW rotation.). As the domain wall velocity is $v = \beta u/\alpha$ below the Walker limit and approaches u when the current density is well above the Walker limit, we can expect that the domain wall velocity will decrease right above the Walker limit when $\beta > \alpha$. Vice

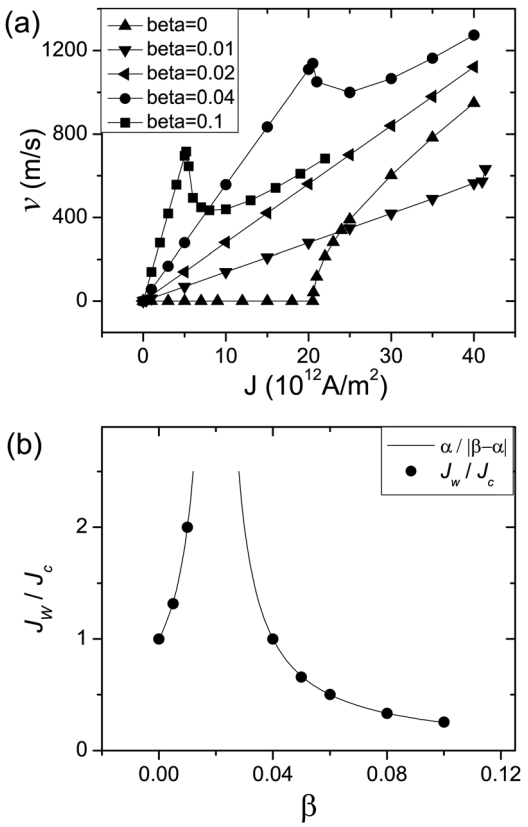

FIG. 5. (a) DW velocity as a function of current density for different β for a rectangular wire. The width is 16 nm and the thickness is 2 nm. (b) Walker breakdown current density as a function β. The solid line is the curve of $J_w/J_c = \alpha/|\beta - \alpha|$ while the solid symbols are the simulated results from (a).

versa, when $\beta < \alpha$, it will increase right above the Walker limit. These explain the simulated results shown in Fig. 5(a). Our simulation also agree with the experimental observation by Hayashi *et al.*,[9] as they observed that the domain wall velocity is above the expected u accompanied by the velocity decrease right above the Walker limit.

The Walker limit for different β can be estimated if we know the maximum difference between v and u. It should be proportional to the maximum value of the procession term. As discussed above, the DW movement has a threshold current J_c when $\beta = 0$. This current can also be considered as the Walker limit J_0 for $\beta = 0$. It is proportional to the maximum precession term. If we define an effective velocity u_0 as the maximum amplitude the precession term that can influence the DW movement, it is proportional to J_0, i.e., J_c. With this, we can derive the condition for obtaining the Walker break point: $|v_w - u_w| = u_0$, where v_w is the Walker threshold velocity. With $v_w = \beta/\alpha u_w$, we can easily derive that $u_w/u_0 = \alpha/|\beta - \alpha|$. As u is proportional to J, we can obtain

$$J_w/J_c = \alpha/|\beta - \alpha|, \tag{4}$$

where J_w is the Walker threshold current density. The Walker threshold current density for different values of β can be obtained from the simulated current dependent DW velocity curve as plotted in Fig. 5(a). The results are plotted in Fig. 5(b). The symbols stand for the simulated results while the solid line is the theoretical curve with the simulated J_c. One can find that the simulated results fit very well with the theoretical curve described by Eq. (4). This result is also consistent with the analytical calculation within one dimension model.[33]

The DW dynamics of a square cross-section wire could be different to that of a rectangular cross-section wire as the threshold current J_c density is much smaller. Fig. 6 shows the simulated DW velocity as a function of the current density for 3 different values of β for a wire of 16 nm thick and 16 nm wide. We can find that all the 3 curves are identical. They linearly increase with the current density, and their slopes are the same and independent with β. This, for the first glimpse, is in sharp contrast with the results obtained from a common rectangular wire as showed in Fig. 5(a). It, however, can be understood if we remember the threshold current J_c for a square wire is in the order of 10^6 A/cm^2 (see Fig. 4) which is much smaller than the currents we used for the calculation. As discussed above, when the applied current is well above the Walker limit, the domain wall velocity will approach to u. Besides moving forward, the DW also rotates around the wire axis. The angular velocity depends on the difference between β and α. Therefore, it can also be used to determine the nonadiabatic parameter β, as proposed by Yan *et al.*[28] for the cylindrical case.

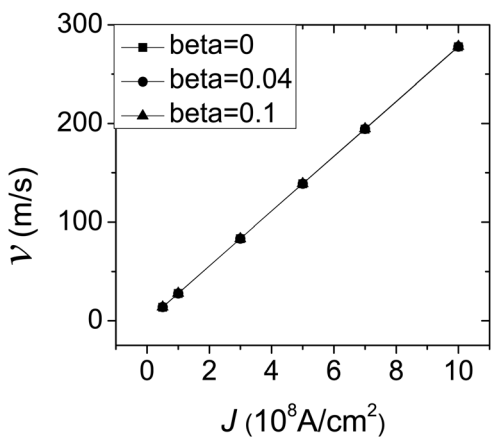

FIG. 6. DW velocity as a function of current density for different β for a square cross-section wire with a thickness of 16 nm.

IV. SUMMARY

We performed micromagnetic simulations of current induced DW motion in Py nanowires. With varying the wire thickness and width, a minimum threshold current in the order of 10^6 A/cm^2 is obtained when the thickness is equivalent to the wire width. With the nonadiabatic spin-transfer term, the calculated domain wall velocity v equals to the adiabatic spin transfer velocity u when the current is far above the Walker limit J_w. Below J_w, $v = \frac{\beta}{\alpha}u$, where β is the nonadiabatic parameter and α is the damping factor. For different β, we find the Walker limit can be scaled as $J_w = \frac{\alpha}{|\beta-\alpha|}J_c$. Our simulations agree well with the one dimensional analytical calculation,[13,33] suggesting the findings are the general behaviors of the systems in this particular geometry.

ACKNOWLEDGMENTS

This work is supported by NSFC (Grants Nos. 10834001, 10874076, 10974087, and 11023002), PAPD and the State Key Programme for Basic Research of China (Grants Nos. 2007CB925104 and 2010CB923401).

[1] L. Berger, Phys. Rev. B **33**, 1572 (1986).
[2] L. Berger, J. Appl. Phys. **63**, 1663 (1988).
[3] S. S. P. Parkin, M. Hayashi, and L. Thomas, Science **320**, 190 (2008).
[4] N. Vernier, D. A. Allwood, D. Atkinson, M. D. Coke, and R. P. Cowburn, Europhys. Lett. **65**, 526 (2004).
[5] A. Yamaguchi, T. Ono, S. Nasu, K. Miyake, K. Mibu, and T. Shinjo, Phys. Rev. Lett. **92**, 077205 (2004).
[6] E. Saitoh, H. Miyajima, T. Yamaoka, and G. Tatara, Nature **432**, 203 (2004).
[7] M. Kläui, P. O. Jubert, R. Allenspach, A. Bischof, J. A. C. Bland, G. Faini, U. Rüdiger, C. A. F. Vaz, L. Vila, and C. Vouille, Phys. Rev. Lett. **95**, 026601 (2005).
[8] M. Kläui, M. Laufenberg, L. Heyne, D. Backes, U. Rüdiger, C. A. F. Vaz, J. A. C. Bland, L. J. Heyderman, S. Cherifi, A., Locatelli, T. O. Mentes, and L. Aballe, Appl. Phys. Lett. **88**, 232507 (2006).
[9] M. Hayashi, L. Thomas, C. Rettner, R. Moriya, B. Bazaliy, and S. P. Parkin, Phys. Rev. Lett. **98**, 037204 (2007).
[10] G. Tatara and H. Kohno, Phys. Rev. Lett. **92**, 086601 (2004).
[11] Z. Li and S. Zhang, Phys. Rev. Lett. **92**, 207203 (2004).
[12] S. Zhang and Z. Li, Phys. Rev. Lett. **93**, 127204 (2004).
[13] A. Thiaville, Y. Nakatani, J. Miltat, and Y. Suzuki, Europhys. Lett. **69**, 990 (2005).
[14] S. E. Barnes and S. Maekawa, Phy. Rev. Lett. **95**, 107204 (2005).
[15] A. Mougin, M. Cormier, J. P. Adam, P. J. Metaxas, and J. Ferré, Europhys. Lett. **78**, 57007 (2007).
[16] M. J. Donahue and D. G. Porter, OOMMF User's Guide, version 1.0, Interagency Report No. NISTIR 6376, National Institute of Standards and Technology, Gaithersburg, MD, 1999 (http://math.nist.gov/oommf/).
[17] OOMMF extension for current-induced domain wall motion developed by IBM research in Zurich, see http://www.zurich.ibm.com/st/magnetism/spintevolve.html.

[18]N. Smith, D. Markham, and D. LaTourette, J. Appl. Phys. **65**, 4362 (1989).
[19]R. J. Soulen, J. M. Byers, M. S. Osofsky, B. Nadgorny, T. Ambrose, S. F. Cheng, P. R. Broussard, C. T. Tanaka, J. Nowak, J. S. Moodera, A. Barry, and J. M. D. Coey, Science **282**, 85 (1998).
[20]J. C. Slonczewski, Int. J. Magn. **2**, 85 (1972).
[21]A. P. Malozemoff and J. C. Slonczewski, *Magnetic Domain Walls in Bubble Materials* (Academic, New York. 1979).
[22]L. Berger, J. Appl. Phys. **49**, 2156 (1978).
[23]A. Kunz and S. C. Reiff, J. Appl. Phys. **103**, 07D903 (2008).
[24]J. Xiao, A. Zangwill, and M. D. Stiles, Phys. Rev. B **73**, 054428 (2006).
[25]A. Vanhaverbeke and M. Viret, Phys. Rev. B **75**, 024411 (2007).
[26]P. Bruno, Phys. Rev. Lett. **83**, 2425 (1999).
[27]Z. J. Yang, L. Sun, X. P. Zhang, M. Cao, X. Y. Deng, A. Hu, and H. F. Ding, Appl. Phys. Lett. **94**, 062514 (2009).
[28]M. Yan, A. Kákay, S. Gliga, and R. Hertel, Phys. Rev. Lett. **104**, 057201 (2010).
[29]T. Koyama, D. Chiba, K. Ueda, K. Kondou, H. Tanigawa, S. Fukami, T. Suzuki, N. Ohshima, N. Ishiwata, Y. Nakatani, K. Kobayashi, and T. Ono, Nature Mater. **10**, 194 (2011).
[30]G. S. D. Beach, C. Nistor, C. Knutsom, M. Tsoi, and J. L. Erskine, Nature Mater. **4**, 741 (2005).
[31]M. Hayashi, L. Thomas, C. Rettner, R. Moriya, and S. S. P. Parkin, Nat. Phys. **3**, 21 (2007).
[32]N. L. Schryer and L. R. Walker, J. Appl. Phys. **45**, 5406 (1974).
[33]A. Mougin, M. Cormier, J. P. Adam, P. J. Metaxas, and J. Ferré, Europhys. Lett. **78**, 57007 (2007).